

# Genetic architecture of gene expression regulation across tissues and implication for prediction

*Heather E. Wheeler<sup>1,2</sup>, ..., GTEx Consortium, Nicholas Knoblauch<sup>3</sup>, Nancy J. Cox<sup>4</sup>, Dan L.*

*Nicolae<sup>5</sup>, Hae Kyung Im<sup>5</sup>*

*<sup>1</sup>Department of Biology and <sup>2</sup>Department of Computer Science, Loyola University Chicago, <sup>3</sup>Committee on Genetics, Genomics, and Systems Biology, University of Chicago, <sup>4</sup>Division of Genetic Medicine, Vanderbilt University, <sup>5</sup>Section of Genetic Medicine, Department of Medicine, University of Chicago*

## Abstract

For many complex traits, gene regulation is likely to play a crucial mechanistic role given the consistent enrichment of expression quantitative trait loci (eQTLs) among trait-associated variants. In order to fully harness gene regulation mechanisms in future studies of complex traits, we sought to better understand the underlying genetic architecture of the gene regulation [\[expression?\]](#) traits across multiple tissues taking advantage of the unique resource generated by the GTEx project.

We started by examining the local and distant heritability as well as the sparsity/polygenicity of gene expression traits using 922 sample RNAseq data from DGN. We found that local contribution can be well estimated using mixed effects modeling approaches with 55% of genes being significantly heritable [\[\[this number is much lower than the 80% of genes that had significant eQTL according to Battle et al. How about BSLMM's estimates with LCS>0, did you say that all of them are >0. Maybe we should look into the FDR<0.05 and see whether we can declare a larger number of 'significant' h2 genes\]\]](#). However with this sample size meaningful estimates of distant heritability can only be obtained when strong functional priors

are used to reduce the number of genetic markers.

For moderately heritable genes ( $h^2 > 25\%$ ) BSLMM results indicate that the local genetic architecture is mostly sparse rather than polygenic. For genes with smaller genetic component the results are not conclusive likely due to reduced power. Moreover, lower performance of ridge regression predictors (highly polygenic) further confirms the sparse architecture of heritable genes.

To further elucidate common and tissue specific regulation, we decomposed the expression traits into a component that is common across tissues and a component that is specific to each tissue using a mixed effects modeling approach. We call this approach Orthogonal Tissue Decomposition to emphasize the fact that the tissue specific component is orthogonal to the cross tissue component improving the interpretability of results.

The cross tissue traits yields a larger number of significantly heritable genes (17%) than any of the individual tissue traits ( $< 8.5\%$ ) due to the increased sample size and integration of information across tissues. Cross tissue and all tissue specific expression traits consistent with a sparse architecture as we found in whole blood for DGN [\[check this holds\]](#). [\[do we get any trans  \$h^2 > 0\$  for CT, TW, or TS?\]](#)

In sum, we have systematically examined the genetic architecture of gene expression traits across 40 tissues, computed derived traits to facilitate tissue specificity evaluation, generated prediction models for all of them using the overall robust and optimal elastic net approach, and provide the models as well as  $h^2$  estimates as a public resource for the scientific community.

**TODO:** run the same analysis as DGN to GTEx CT, TW, TS traits and comment of commonalities and differences.

**TODO:** add somewhere in the manuscript, probably not the abstract, that we do not see  $h^2$  dependence on expression level in contrast to what is reported for array based  $h^2$  estimates

**TODO:** plot a) array based  $h^2$  vs. RPKM in gtex, use alkes and or fred wright's  $h^2$  estimates b) RNAseq  $h^2$  vs RPKM in gtex

# Introduction

Regulatory variation has been shown to play a key role in the genetics of complex traits [1–3]. While many common diseases have been shown to be polygenic [4–6], it is unclear whether gene expression levels are also polygenic or instead have simpler genetic architectures and how much these expression architectures vary across genes [7]. Most human expression quantitative trait loci (eQTL) studies have focused on how local genetic variation affects gene expression in order to reduce the multiple testing burden that would be required for a global analysis [7,8]. Furthermore, when both local and distal eQTLs are reported [9–11], effect sizes and replicability are much higher for local eQTLs. Indeed, while the heritability of gene expression attributable to local genetic variation has been estimated accurately, large standard errors have prevented accurate estimation of the contribution of distal genetic variation to gene expression variation [11,12].

Most human eQTL studies have been performed in whole blood or lymphoblastoid cell lines due to ease of access or culturability [9,13,14]. The Genotype-Tissue Expression (GTEx) Project aims to examine the genetics of gene expression more comprehensively and recently published a pilot analysis of RNA sequencing data from 1641 samples across 43 tissues from 175 individuals [15]. In order to better understand the genetic architecture of tissue-specific and cross-tissue gene regulation, we developed a mixed effects model called orthogonal tissue decomposition (OTD) to determine the cross-tissue and tissue-specific components of gene expression in the rich GTEx dataset. These components were used to develop predictors of cross-tissue and tissue-specific gene expression for use in our gene-based association method PrediXcan [16].

We also assessed the ability of various models with different underlying assumptions to predict gene expression in order to understand the underlying genetic architecture of gene expression. Gene expression traits with sparse architecture should be better predicted with sparse models such as LASSO (Least Absolute Shrinkage and Selection Operator) [17] while highly polygenic traits should be better predicted with ridge regression or similarly polygenic models [18–20]. Using the hybrid approach of BSLMM (Bayesian Sparse Linear Mixed Model) [21], we quantified the proportion of the sparse component that makes up the total proportion of expression variance explained by sparse and polygenic effects.

Specifically, in this paper we show that local heritability can be accurately estimated across tissues, but distal

heritability cannot reliably estimated at current sample sizes. We also show that for local gene regulation, the genetic architecture is mostly sparse rather than polygenic. We found that estimates of the local heritability of cross-tissue gene expression generated with our OTD model have larger magnitude and improved standard errors compared to single tissue estimates due to the borrowing of information across all samples. Comparing our OTD results to a previously performed joint multi-tissue eQTL analysis method [22], we show that genes with high cross-tissue heritability are more likely to have cross-tissue eQTLs, confirming that OTD is capturing the cross-tissue component of gene expression. We also found evidence that genes with large tissue-specific heritability are enriched in common complex disease genes discovered via GWAS. [[Redo with PVE estimates from BSLMM]]

## Results

### Local genetic variation explains a large proportion of gene expression variance

We estimated the heritability of gene expression in whole blood from the Depression Genes and Networks (DGN) cohort (n=922) [14] using a mixed-effects model (see Methods) and calculated variances using restricted maximum likelihood as implemented in GCTA [23]. We fit a joint model with a local and a distal genetic relationship matrix (GRM). The local GRM was derived from SNPs within 1 Mb of each gene and the distal GRM was derived from SNPs that are located on non-gene chromosomes and are eQTLs in the Framingham Heart Study (FHS) cohort (n=5257, FDR < 0.05) [24]. The mean local  $h^2$  was 0.130 and 54.6% of genes had a positive 95% confidence interval (CI), while the mean distal  $h^2$  was 0.076 and just 4.2% of genes had a positive CI (Fig 1). The maximum local  $h^2$  was 0.93 with a standard error (SE) of 0.009 while the maximum distal  $h^2$  was 0.91 with a SE of 0.16. Similar results were observed for the 1194 genes with *trans*-eQTLs (FHS FDR < 0.05) when the distal GRM was limited to known *trans*-eQTLs (Fig 2). That is, the mean local  $h^2$  was 0.133 and 61.3% of genes had a positive 95% confidence interval (CI), while the mean *trans*  $h^2$  was just 0.021 and 4.2% of genes tested had a positive CI.

## **The effect of local genetic variation on gene expression is sparse rather than polygenic**

We performed 10-fold cross-validation using the elastic net [25] to test the predictive performance of local SNPs for gene expression across a range of mixing parameters,  $\alpha$ . The  $\alpha$  that gives the largest cross-validation  $R^2$  informs the sparsity of each gene expression trait. That is, at one extreme, if the optimal  $\alpha = 0$  (equivalent to ridge regression), the gene expression trait is highly polygenic, whereas if the optimal  $\alpha = 1$  (equivalent to LASSO), the trait is highly sparse. We found that for most gene expression traits, the cross-validated  $R^2$  was suboptimal for  $\alpha = 0$  and  $\alpha = 0.05$ , but nearly identically optimal for  $\alpha = 0.5$  and  $\alpha = 1$  in the DGN cohort (Fig 3). This suggests that for most genes, the effect of local genetic variation on gene expression is sparse rather than polygenic.

To further examine sparsity and polygenicity, we used BSLMM [21] to define the total proportion of variance in expression explained by sparse and polygenic effects together (PVE) and the proportion of this genetic variance explained by sparse effects (PGE) for each gene in the DGN cohort. The PVE can be thought of as a Bayesian estimate of chip heritability and, indeed, there is a strong correlation between BSLMM-estimated PVE and GCTA-estimated  $h^2$  (Fig 4A,  $R=0.96$ ). For genes with large PVE, the PGE also was large, indicative of a sparse genetic architecture. For example, all genes with  $PVE > 0.50$  had  $PGE > 0.82$  and their median PGE was 0.989 (Fig 4B). The median PGE for genes with  $PVE > 0.1$  was 0.949. Fittingly, for most (96.3%) of the genes with PVE estimates  $> 0.10$ , the median number of SNPs included in the model was no more than 10 (Fig 4C).

## **Cross-tissue and tissue-specific gene expression by orthogonal tissue decomposition**

In order to better understand the context specificity of gene expression regulation, we developed a method called orthogonal tissue decomposition (OTD), which uses a mixed effects model to generate cross-tissue and tissue-specific gene expression levels (see Methods). Using a marginal model with just the local GRM, we estimated the local  $h^2$  of cross-tissue gene expression and tissue-specific gene expression in the nine tissues

with the most samples. The cross-tissue heritabilities were larger and the standard errors were smaller than the tissue-specific estimates (Fig 5). The percentage of  $h^2$  estimates with positive CIs was much larger for cross-tissue expression (17.3%) than the tissue-specific expressions (all less than 3%, Fig 6).

We also compared the cross-tissue  $h^2$  from the OTD to  $h^2$  estimates from the pre-OTD measures of gene expression in each of the nine tissues, which we term tissue-wide expression. Again, the cross-tissue heritabilities were larger and the standard errors were smaller than the tissue-wide estimates (Fig 7), though less striking than the tissue-specific comparison. The percentage of tissue-wide  $h^2$  estimates with positive CIs ranged from 4.4-8.6% and thus were all larger than the tissue-specific positive CI percentages, but smaller than the cross-tissue percentage (Fig 8).

We compared our OTD results to those from a joint multi-tissue eQTL analysis method [22], which was previously performed on a subset of the GTEx data [15]. The results of this analysis include eQTL posterior probabilities for each of the nine tissues, which can be interpreted as the probability a SNP is an eQTL in tissue  $x$  given the data. Using the top eQTL for each gene, we defined an entropy statistic (see Methods) that combines the nine posterior probabilities into one value such that higher entropy values mean the gene is more likely to be regulated by the same eQTL across all nine tissues, rather than in just a subset of the nine. We observed a strong correlation between entropy and both the cross-tissue expression heritability ( $R = 0.082$ , Fig 9A) and PVE ( $R = 0.12$ , Fig 9B) estimates, using the cross-tissue expression derived from the OTD. Thus, genes with high cross-tissue heritability are more likely to have cross-tissue eQTLs, confirming that OTD is capturing the cross-tissue component of gene expression. Also, the correlation between tissue-specific OTD gene expression PVE and the posterior probability that the gene has an eQTL in that tissue is strongest in each respective tissue, confirming that OTD also captures tissue-specific components of gene expression (Fig 10).

## Discussion

Because regulatory variation plays a key mechanistic role in the genetics of complex traits [1–3], we sought to comprehensively characterize the genetic architecture of gene expression across tissues. We show that the

local architecture of gene expression is sparse for 95% of heritable genes and that distal architecture cannot be accurately assessed at current sample sizes ( $n < 1000$ ). [[compare mean  $h^2$ 's across studies]] Indeed, while the heritability of gene expression attributable to local genetic variation has been estimated accurately, large standard errors have prevented accurate estimation of the contribution of distal genetic variation to gene expression variation [11,12].

We developed a mixed effects model called orthogonal tissue decomposition (OTD) to determine the cross-tissue and tissue-specific components of gene expression in the rich GTEx dataset. These components were used to develop predictors of cross-tissue and tissue-specific gene expression for use in our gene-based association method PrediXcan [16]. The tissue availability is unbalanced because of the difficulties of sample collection and the uneven quality of the tissues. Furthermore, by using a mixed effects model to create cross-tissue expression, we borrow information across tissues, which should increase our power to detect associations and achieve better predictive models.

We also assessed the ability of various models with different underlying assumptions to predict gene expression in order to understand the underlying genetic architecture of gene expression. Gene expression traits with sparse architecture should be better predicted with sparse models such as LASSO (Least Absolute Shrinkage and Selection Operator) [17] while highly polygenic traits should be better predicted with ridge regression or similarly polygenic models [18–20]. Using the hybrid approach of BSLMM (Bayesian Sparse Linear Mixed Model) [21], we quantified the proportion of the sparse component that makes up the total proportion of expression variance explained by sparse and polygenic effects.

Specifically, in this paper we show that local heritability can be accurately estimated across tissues, but distal heritability cannot reliably estimated at current sample sizes. We also show that for local gene regulation, the genetic architecture is mostly sparse rather than polygenic. We found that estimates of the local heritability of cross-tissue gene expression generated with our OTD model have larger magnitude and improved standard errors compared to single tissue estimates due to the borrowing of information across all samples. Comparing our OTD results to a previously performed joint multi-tissue eQTL analysis method [22], we show that genes with high cross-tissue heritability are more likely to have cross-tissue eQTLs, confirming that OTD is capturing the cross-tissue component of gene expression.

The tissue availability is unbalanced because of the difficulties of sample collection and the uneven quality of the tissues. Furthermore, by using a mixed effects model to create cross-tissue expression, we borrow information across tissues, which should increase our power to detect associations and achieve better predictive models.

## Methods

### Genomic and Transcriptomic Data

#### DGN Dataset

We obtained whole blood RNA-Seq and genome-wide genotype data for 922 individuals from the Depression Genes and Networks (DGN) cohort [14], all of European ancestry. For our analyses, we used the HCP (hidden covariates with prior) normalized gene-level expression data used for the *trans*-eQTL analysis in Battle et al. [14] and downloaded from the NIMH repository. The 922 individuals were unrelated (all pairwise  $\hat{\pi} < 0.05$ ) and thus all included in downstream analyses. Imputation of approximately 650K input SNPs (minor allele frequency [MAF]  $> 0.05$ , Hardy-Weinberg Equilibrium [ $P > 0.05$ ], non-ambiguous strand [no A/T or C/G SNPs]) was performed on the University of Michigan Imputation-Server (<https://imputationserver.sph.umich.edu/start.html>) [26,27] with the following parameters: 1000G Phase 1 v3 ShapeIt2 (no singletons) reference panel, SHAPEIT phasing, and EUR population. Approximately 1.9M non-ambiguous strand SNPs with MAF  $> 0.05$ , imputation  $R^2 > 0.8$  and, to reduce computational burden, inclusion in HapMap Phase II were retained for subsequent analyses.

#### GTEx Dataset

We obtained RNA-Seq gene expression levels from 8555 tissue samples (53 unique tissue types) from 544 unique subjects in the GTEx Project [15] data release on 2014-06-13. Of the individuals with gene expression data, genome-wide genotypes (imputed with 1000 Genomes) were available for 450 individuals. While all 8555 tissue samples were used in the OTD model (described below) to generate cross-tissue and tissue-specific



components of gene expression, we used the nine tissues with the largest sample sizes when quantifying tissue-specific effects. Tissues and sample sizes (both RNA-seq and genotypes available) included cross-tissue ( $n = 450$ ), skeletal muscle ( $n = 361$ ), whole blood ( $n = 339$ ), skin from the sun-exposed portion of the lower leg ( $n = 303$ ), subcutaneous adipose ( $n = 298$ ), tibial artery ( $n = 285$ ), lung ( $n = 279$ ), thyroid ( $n = 279$ ), tibial nerve ( $n = 256$ ) and left ventricle heart ( $n = 190$ ). Approximately 2.6M non-ambiguous strand SNPs included in HapMap Phase II were retained for subsequent analyses.

## Partitioning local and distal heritability of gene expression

To investigate the proximity of gene expression regulation to each gene, we partitioned the proportion of gene expression variance explained by SNPs in the DGN cohort into two components: local (SNPs within 1Mb of the gene) and distal (eQTLs on non-gene chromosomes) as defined by the GENCODE [28] version 12 gene annotation. We calculated the proportion of the variance (narrow-sense heritability) explained by each component using the following mixed-effects model:

$$Y_g = \sum_{k \in local} w_{k,g} X_k + \sum_{k \in distal} w_{k,g} X_k + \epsilon$$

Assuming a random effects for  $w_{k,g} \approx N(0, \sigma_w^2)$  and  $\epsilon \approx N(0, \sigma_\epsilon^2 I_n)$ , where  $I_n$  is the identity matrix, we calculated the total variability explained by local and distal components by estimating  $\sigma_w^2$  with restricted maximum likelihood (REML) using GCTA software [23]. For heritability analyses in the GTEx cohort, we removed the *distal* term from the model and only estimated marginal *local*  $h^2$  due to the smaller sample sizes of both cross-tissue and tissue-specific expression levels compared to DGN.

## Determining polygenicity versus sparsity using the elastic net

We applied the elastic net [25] to model the effect of local genetic variation (SNPs within 1 Mb of gene) on the genetic architecture of gene expression. We used the `cv.glmnet` function in the R package `glmnet` [29,30] to perform 10-fold cross-validation of the elastic net across a range of mixing parameters ( $\alpha$ ) to find the  $\alpha$

that maximized predictive performance, measured by Pearson’s  $R^2$ . Specifically, `glmnet` solves the following problem:

[[Haky, should/can we simplify this equation? I just took it from [http://web.stanford.edu/~hastie/glmnet/glmnet\\_alpha.html](http://web.stanford.edu/~hastie/glmnet/glmnet_alpha.html), but they don’t explain all the terms]]

$$\min_{\beta_0, \beta} \frac{1}{N} \sum_{i=1}^N w_i l(y_i, \beta_0 + \beta^T x_i) + \lambda \left[ (1 - \alpha) \|\beta\|_2^2 / 2 + \alpha \|\beta\|_1 \right],$$

over a grid of values of  $\lambda$  covering the entire range [29,30]. This tuning parameter  $\lambda$  controls the overall strength of the penalty.

The elastic net penalty is controlled by mixing parameter  $\alpha$ , which spans LASSO ( $\alpha = 1$ , the default) [17] at one extreme and ridge regression ( $\alpha = 0$ ) [18] at the other. The ridge penalty shrinks the coefficients of correlated SNPs towards each other, while the LASSO tends to pick one of the correlated SNPs and discard the others. Thus, an optimal prediction  $R^2$  for  $\alpha = 0$  means the gene expression trait is highly polygenic, while an optimal prediction  $R^2$  for  $\alpha = 1$  means the trait is highly sparse. An optimal prediction  $R^2$  in between (e.g.  $\alpha = 0.5$ ) means the trait has a mixed genetic architecture.

In the DGN cohort, we tested 21 values of the mixing parameter ( $\alpha = 0, 0.05, 0.1, \dots, 0.90, 0.95, 1$ ) for optimal prediction of gene expression of the 341 genes on chromosome 22. For the rest of the autosomes in DGN and for cross-tissue, tissue-specific, and tissue-wide expression in the GTEx cohort, we tested  $\alpha = 0.05, 0.5, 0.95, 1$ .  
[[add when finished, need to do DGN alpha=0.05 and 0.95]]

## Quantifying sparsity with Bayesian Sparse Linear Mixed Models (BSLMM)

We used BSLMM [21] to model the effect of local genetic variation (SNPs within 1 Mb of gene) on the genetic architecture of gene expression. The BSLMM consists of a standard linear mixed model, with one random effect term, and with sparsity inducing priors on the regression coefficients [21]. We used the software GEMMA [31] to implement BSLMM for each gene using the following parameters:

```
gemma -g [localGenoFile] -p [geneExpFile] -a [snpAnnotFile] -bslmm 1 -s 100000 -o [outFile]
```

The `-bslmm 1` option specifies a linear BSLMM and the `-s 100000` option specifies the number of sampling steps per gene. The BSLMM estimates the PVE (the total proportion of variance in phenotype explained by the sparse effects and random effects terms together) and PGE (the proportion of genetic variance explained by the sparse effects terms). From the second half of the sampling iterations for each gene, we report the median and the 95% credible sets of the PVE, PGE, and the  $|\gamma|$  parameter (the number of SNPs with non-zero coefficients).

## Orthogonal tissue decomposition

To better understand the context specificity of gene expression regulation, we developed a method called orthogonal tissue decomposition (OTD). This approach is an extension of our method to develop an intrinsic growth phenotype [32]. We applied OTD to GTEx Project [15] data and decomposed the expression of each gene into cross-tissue and tissue-specific components. The tissue availability is unbalanced across individuals because of the difficulties of sample collection and the uneven quality of the tissues. OTD decomposes the expression traits into orthogonal components as represented by the following model:

$$Y_i = T_{i,cross} + T_{i,tissue}$$

Specifically, to generate cross-tissue and tissue-specific expression levels, we used the `lmer` function in the R [33] package `lme4` [34,35] to fit the following mixed-effects model:

```
fit <- lme4::lmer(expression ~ (1|SUBJID) + TISSUE + GENDER + PEERs)
```

The model included tissue-wide gene expression levels in 8555 GTEx tissue samples from 544 unique subjects. A total of 17,647 Protein-coding genes (defined by GENCODE [28] version 18) with a mean gene expression level across tissues greater than 0.1 RPKM (reads per kilobase of transcript per million reads mapped) were included in the model. `SUBJID` was a random effect and the covariates `TISSUE`, `GENDER`, and `PEERs` were

fixed effects used to predict tissue-wide expression levels (`expression` in the model). PEERs included the top 15 PEER factors estimated across all tissues using the R package PEER [36] to control for batch effects and experimental confounders. Cross-tissue expression was defined as the random effects from the model (`ranef(fit)`) and tissue-specific expression as the residuals (`resid(fit)`).

## Comparison of OTD PVE to multi-tissue eQTL results

Using results from a joint multi-tissue eQTL analysis method [22] performed with a subset of the GTEx data (maximum  $n=175$  in the nine tissues of the pilot phase, see [15]), we defined an entropy statistic to compare these results to those from our OTD method. The results of the multi-tissue analysis include eQTL posterior probabilities for each of the nine tissues, which can be interpreted as the probability a SNP is an eQTL in tissue  $t$  given the data. Using the top eQTL for each gene  $g$ , we defined the entropy  $S_g$  as:

$$S_g = - \sum_t p_{t,g} \log p_{t,g}$$

where  $p_{t,g}$  is the eQTL probability in tissue  $t$  normalized to 1 for each gene  $g$ . Thus, eQTLs with higher entropy statistics are more likely to be cross-tissue eQTLs, rather than only regulating gene expression in one or a few tissues. We calculated the Pearson correlation between  $S_g$  and the cross-tissue expression heritability and PVE for each gene to verify that our OTD method captures cross-tissue effects. We also calculated a Pearson correlation matrix between the posterior probabilities in each tissue from the multi-tissue eQTL method and the tissue-specific gene expression PVE from the OTD method.

## Enrichment analysis

- For top CT and TS genes:
  1. GO enrichment
  2. GWAS catalog enrichment (i.e. top T2D, T1D, schizo, etc. genes) [[redo GWAS catalog enrichment with CT and TS top PVE]]

**Tables**

**Figures**

**Supplemental Figures**

**References**

1. Nicolae DL, Gamazon E, Zhang W, Duan S, Dolan ME, Cox NJ. Trait-associated SNPs are more likely to be eQTLs: Annotation to enhance discovery from GWAS. Gibson G, editor. PLoS Genetics. Public Library of Science (PLoS); 2010;6: e1000888. doi:[10.1371/journal.pgen.1000888](https://doi.org/10.1371/journal.pgen.1000888)
2. Nica AC, Montgomery SB, Dimas AS, Stranger BE, Beazley C, Barroso I, et al. Candidate causal regulatory effects by integration of expression QTLs with complex trait genetic associations. Gibson G, editor. PLoS Genetics. Public Library of Science (PLoS); 2010;6: e1000895. doi:[10.1371/journal.pgen.1000895](https://doi.org/10.1371/journal.pgen.1000895)
3. Gusev A, Lee SH, Trynka G, Finucane H, Vilhjálmsson BJ, Xu H, et al. Partitioning heritability of regulatory and cell-type-specific variants across 11 common diseases. The American Journal of Human Genetics. Elsevier BV; 2014;95: 535–552. doi:[10.1016/j.ajhg.2014.10.004](https://doi.org/10.1016/j.ajhg.2014.10.004)
4. Purcell SM, Wray NR, Stone JL, Visscher PM, Sullivan MCOPF, Sklar P, et al. Common polygenic variation contributes to risk of schizophrenia and bipolar disorder. Nature. Nature Publishing Group; 2009; doi:[10.1038/nature08185](https://doi.org/10.1038/nature08185)
5. Stahl EA, Wegmann D, Trynka G, Gutierrez-Achury J, Do R, Voight BF, et al. Bayesian inference analyses of the polygenic architecture of rheumatoid arthritis. Nature Genetics. Nature Publishing Group; 2012;44: 483–489. doi:[10.1038/ng.2232](https://doi.org/10.1038/ng.2232)
6. Morris AP, Voight BF, Teslovich TM, Ferreira T, Segrè AV, Steinthorsdottir V, et al. Large-scale association analysis provides insights into the genetic architecture and pathophysiology of type 2 diabetes. Nature Genetics. Nature Publishing Group; 2012;44: 981–990. doi:[10.1038/ng.2383](https://doi.org/10.1038/ng.2383)
7. Albert FW, Kruglyak L. The role of regulatory variation in complex traits and disease. Nat Rev Genet. Nature Publishing Group; 2015;16: 197–212. doi:[10.1038/nrg3891](https://doi.org/10.1038/nrg3891)

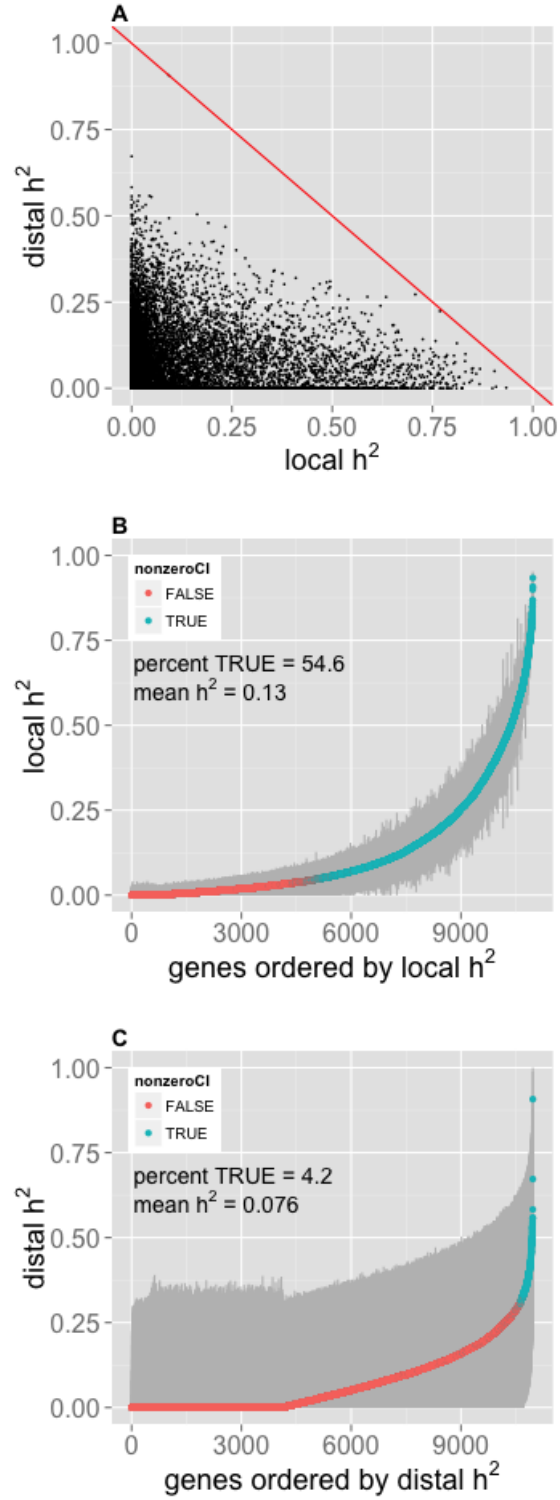


Figure 1: DGN whole blood expression joint heritability ( $h^2$ ). Local (SNPs within 1 Mb of each gene) and distal (SNPs that are eQTLs in the Framingham Heart Study on other chromosomes [FDR < 0.05])  $h^2$  for gene expression were jointly estimated. **(A)** Distal  $h^2$  compared to local  $h^2$  per gene. **(B)** Local and **(C)** distal gene expression  $h^2$  estimates ordered by increasing  $h^2$ . The 95% confidence interval (CI) of each  $h^2$  estimate is in gray and genes with a lower bound greater than zero are in blue.

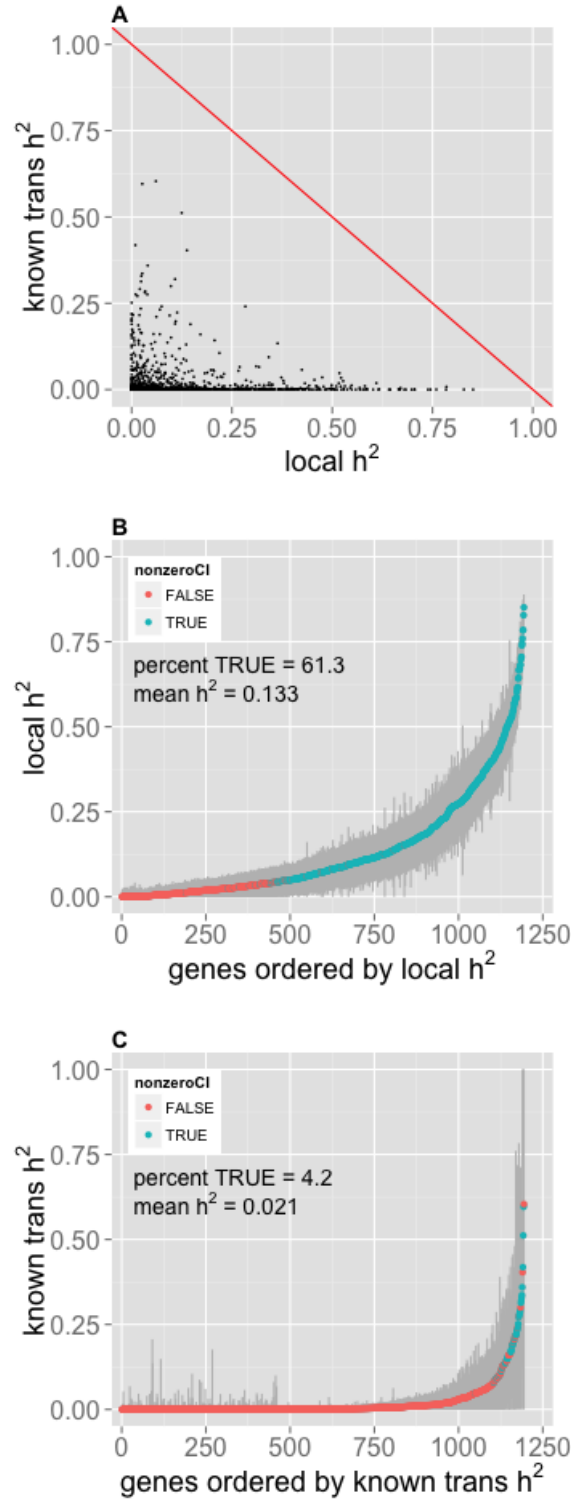


Figure 2: DGN whole blood expression joint heritability ( $h^2$ ) with known trans-eQTLs. Local (SNPs within 1 Mb of each gene) and known trans (SNPs that are trans-eQTLs in the Framingham Heart Study for each gene [FDR < 0.05])  $h^2$  for gene expression were jointly estimated. **(A)** Known trans  $h^2$  compared to local  $h^2$  per gene. **(B)** Local and **(C)** known trans gene expression  $h^2$  estimates ordered by increasing  $h^2$ . The 95% confidence interval (CI) of each  $h^2$  estimate is in gray and genes with a lower bound greater than zero are in blue.

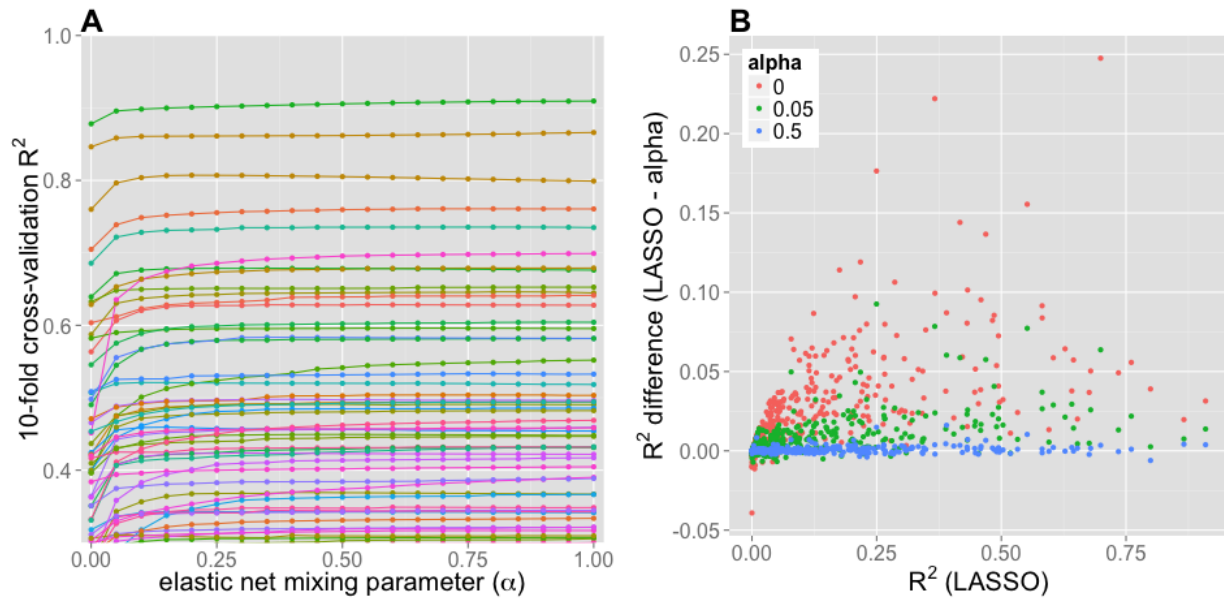


Figure 3: Cross-validated predictive performance across the elastic net. (A) 10-fold cross-validated  $R^2$  of predicted vs. observed expression in DGN whole blood compared to a range of elastic net mixing parameters ( $\alpha$ ) for genes on chromosome 22 with  $R^2 > 0.3$ . (B) Predictive  $R^2$  difference between LASSO ( $\alpha = 1$ ) and several other values of  $\alpha$  compared to LASSO predictive  $R^2$  for 341 genes on chromosome 22.

8. Stranger BE, Montgomery SB, Dimas AS, Parts L, Stegle O, Ingle CE, et al. Patterns of cis regulatory variation in diverse human populations. Barsh GS, editor. PLoS Genetics. Public Library of Science (PLoS); 2012;8: e1002639. doi:[10.1371/journal.pgen.1002639](https://doi.org/10.1371/journal.pgen.1002639)
9. Stranger BE, Nica AC, Forrest MS, Dimas A, Bird CP, Beazley C, et al. Population genomics of human gene expression. Nature Genetics. Nature Publishing Group; 2007;39: 1217–1224. doi:[10.1038/ng2142](https://doi.org/10.1038/ng2142)
10. Innocenti F, Cooper GM, Stanaway IB, Gamazon ER, Smith JD, Mirkov S, et al. Identification, replication, and functional fine-mapping of expression quantitative trait loci in primary human liver tissue. Storey JD, editor. PLoS Genetics. Public Library of Science (PLoS); 2011;7: e1002078. doi:[10.1371/journal.pgen.1002078](https://doi.org/10.1371/journal.pgen.1002078)
11. Wright FA, Sullivan PF, Brooks AI, Zou F, Sun W, Xia K, et al. Heritability and genomics of gene expression in peripheral blood. Nature Genetics. Nature Publishing Group; 2014;46: 430–437. doi:[10.1038/ng.2951](https://doi.org/10.1038/ng.2951)
12. Price AL, Helgason A, Thorleifsson G, McCarroll SA, Kong A, Stefansson K. Single-tissue and cross-tissue heritability of gene expression via identity-by-descent in related or unrelated individuals. Gibson G, editor. PLoS Genetics. Public Library of Science (PLoS); 2011;7: e1001317. doi:[10.1371/journal.pgen.1001317](https://doi.org/10.1371/journal.pgen.1001317)



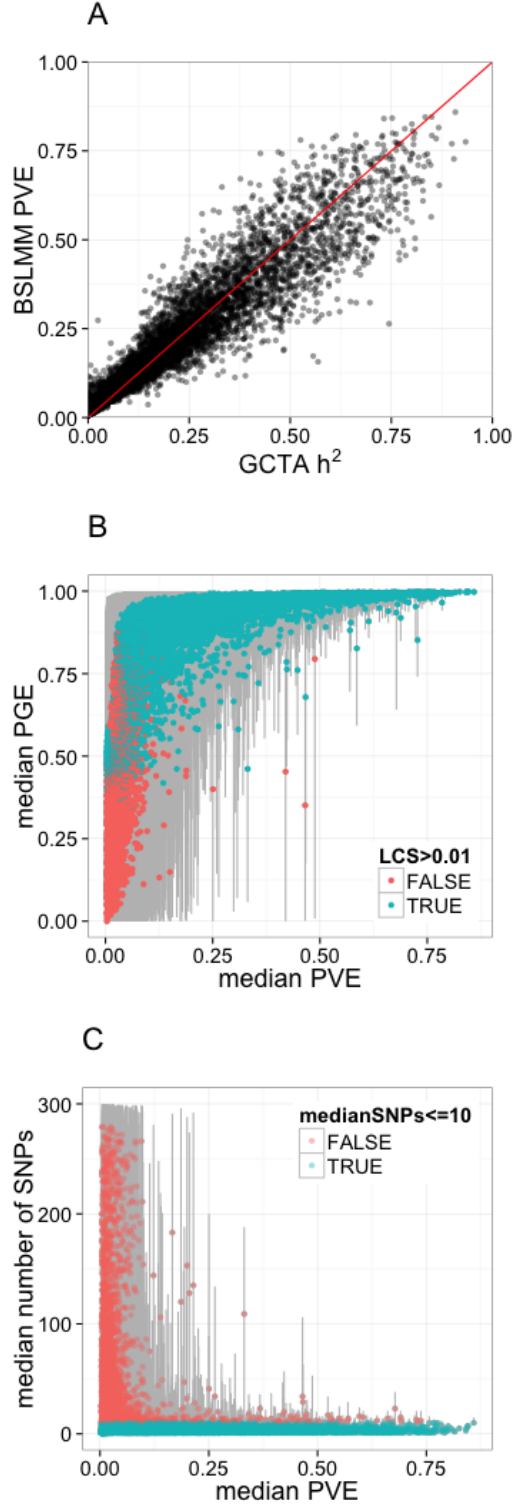


Figure 4: Bayesian Sparse Linear Mixed Models reveal the sparsity of gene expression architecture. **(A)** BSLMM-estimated PVE (total proportion of variance explained) compared to GCTA-estimated heritability per gene ( $R=0.96$ ) **(B)** Comparison of median PGE (proportion of PVE explained by sparse effects) to median PVE (total proportion of variance explained) for expression of each gene. The 95% credible set of each PGE estimate is in gray and genes with a lower credible set (LCS) greater than 0.01 are in blue. **(C)** Comparison of the median number of SNPs included in the model of each gene to median PVE. The 95% credible set of each SNP-number estimate is in gray and genes with a median of 10 or fewer SNPs are in blue.

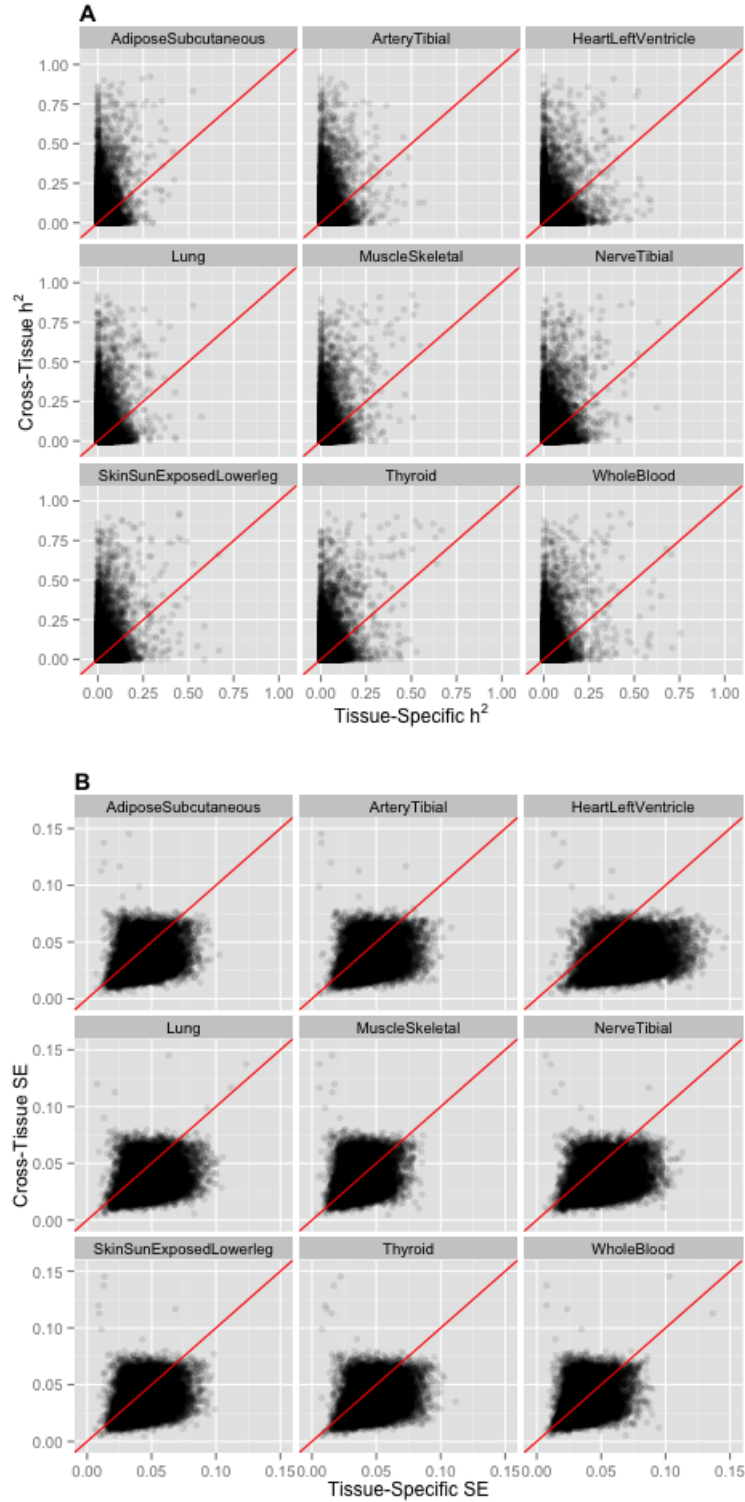


Figure 5: Cross-tissue and tissue-specific comparison of heritability ( $h^2$ , **A**) and standard error (SE, **B**) estimation. Cross-tissue local  $h^2$  is estimated using the cross-tissue component (random effects) of the mixed effects model for gene expression and SNPs within 1 Mb of each gene. Tissue-specific local  $h^2$  is estimated using the tissue-specific component (residuals) of the mixed effects model for gene expression for each respective tissue and SNPs within 1 Mb of each gene.

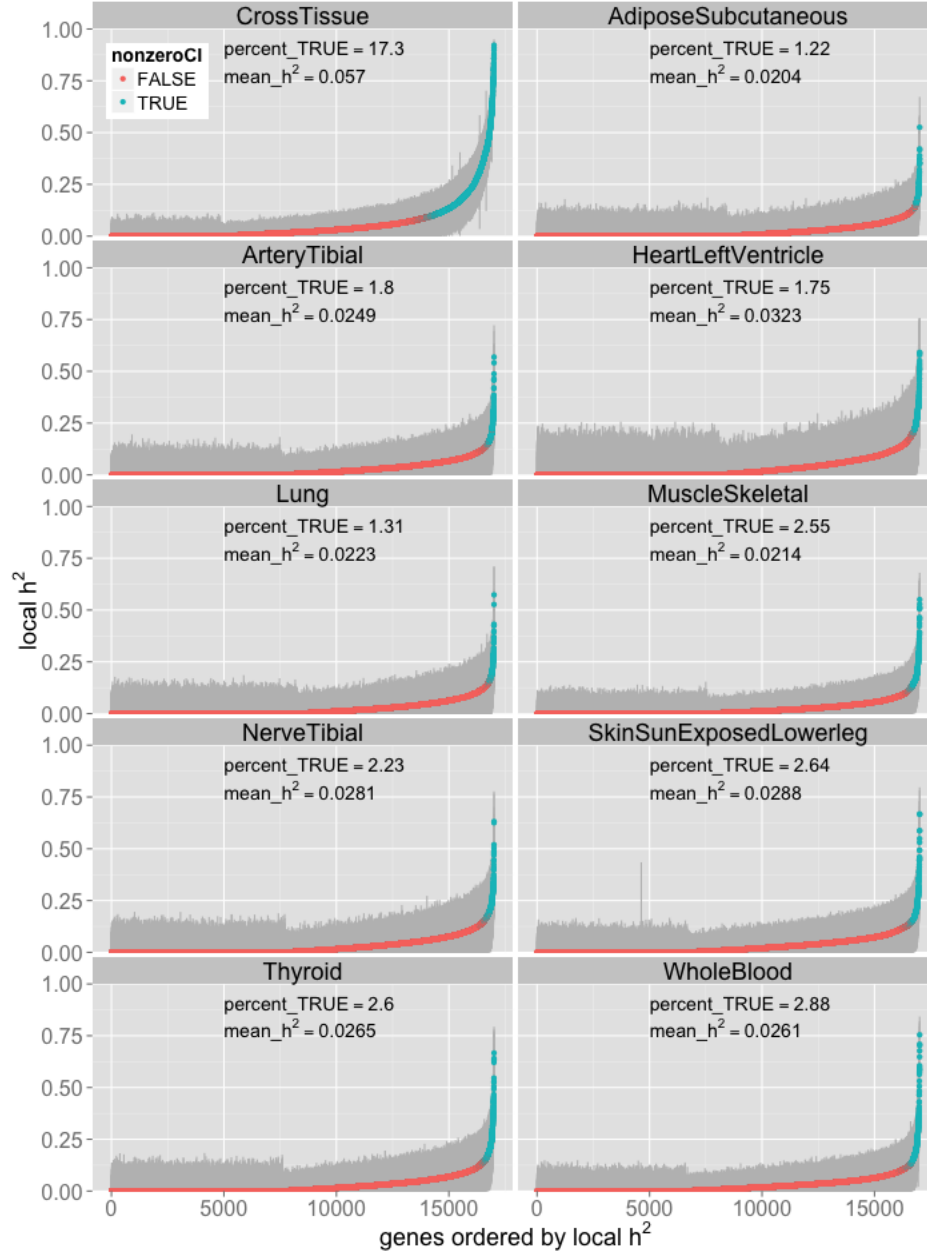


Figure 6: Cross-tissue heritability ( $h^2$ ) compared to tissue-specific  $h^2$ . Cross-tissue local  $h^2$  is estimated using the cross-tissue component (random effects) of the mixed effects model for gene expression and SNPs within 1 Mb of each gene. Tissue-specific local  $h^2$  is estimated using the tissue-specific component (residuals) of the mixed effects model for gene expression for each respective tissue and SNPs within 1 Mb of each gene.

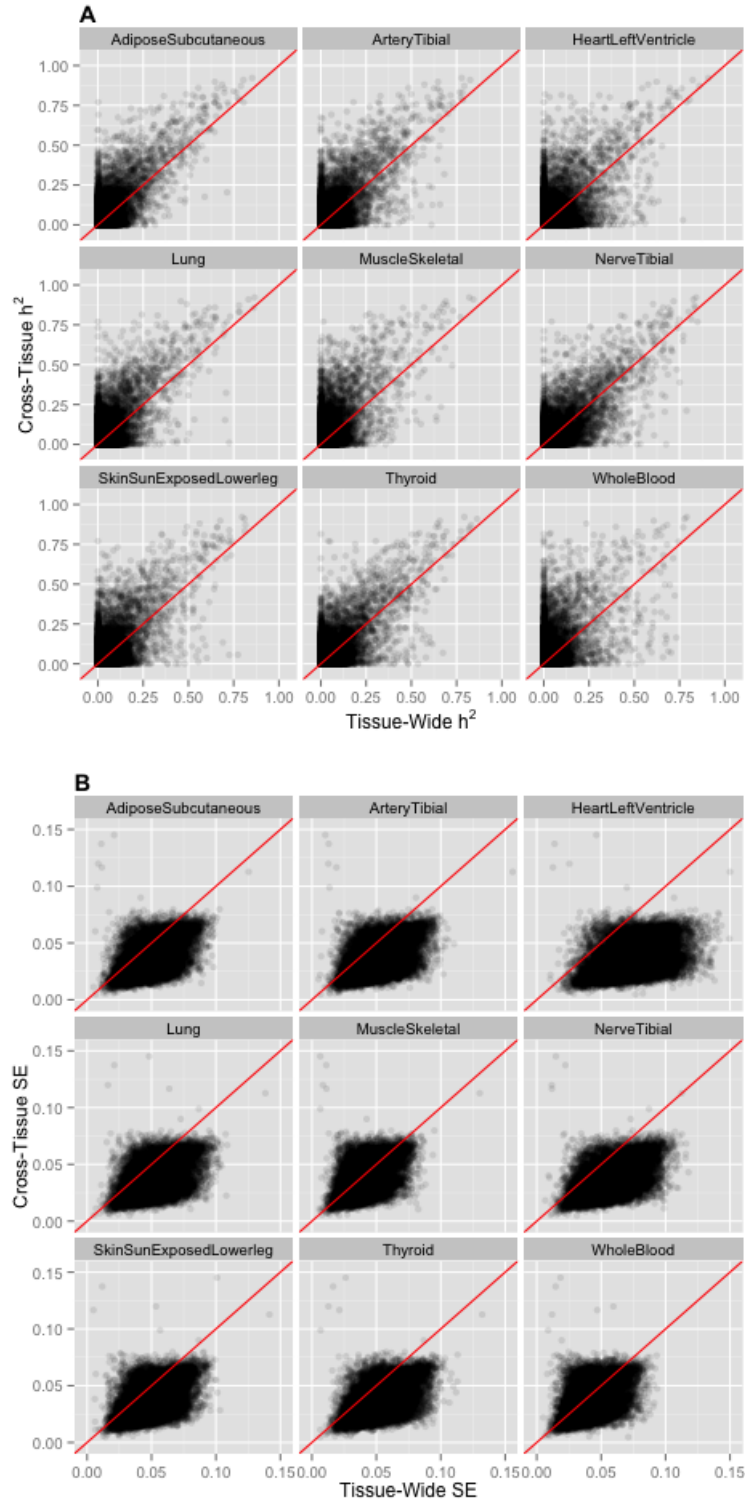


Figure 7: Cross-tissue and tissue-wide comparison of heritability ( $h^2$ , **A**) and standard error (SE, **B**). Cross-tissue local  $h^2$  is estimated using the cross-tissue component (random effects) of the mixed effects model for gene expression and SNPs within 1 Mb of each gene. Tissue-wide local  $h^2$  is estimated using the measured gene expression for each respective tissue and SNPs within 1 Mb of each gene.

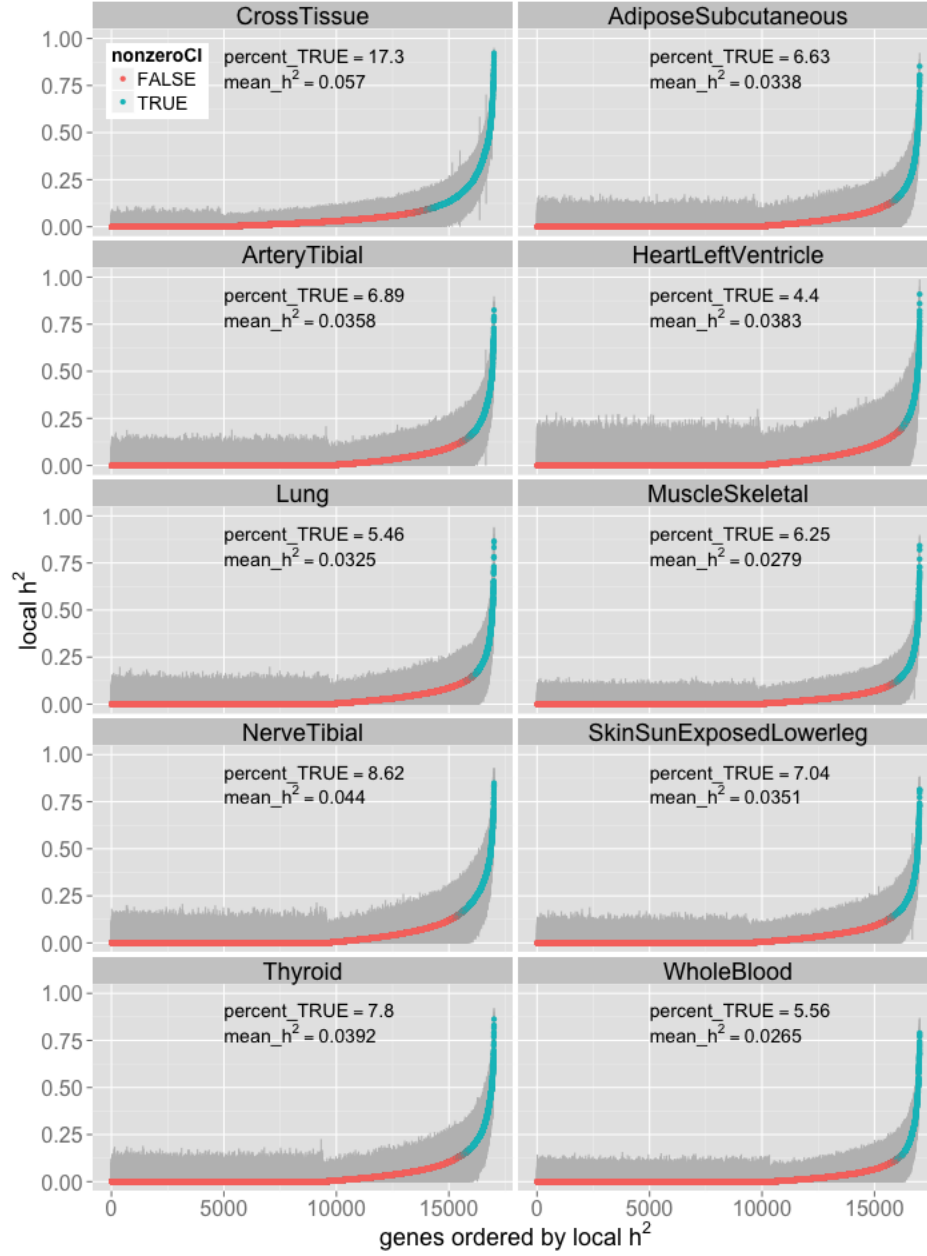


Figure 8: Cross-tissue heritability ( $h^2$ ) compared to tissue-wide  $h^2$ . Cross-tissue local  $h^2$  is estimated using the cross-tissue component (random effects) of the mixed effects model for gene expression and SNPs within 1 Mb of each gene. Tissue-wide local  $h^2$  is estimated using the measured gene expression for each respective tissue and SNPs within 1 Mb of each gene.

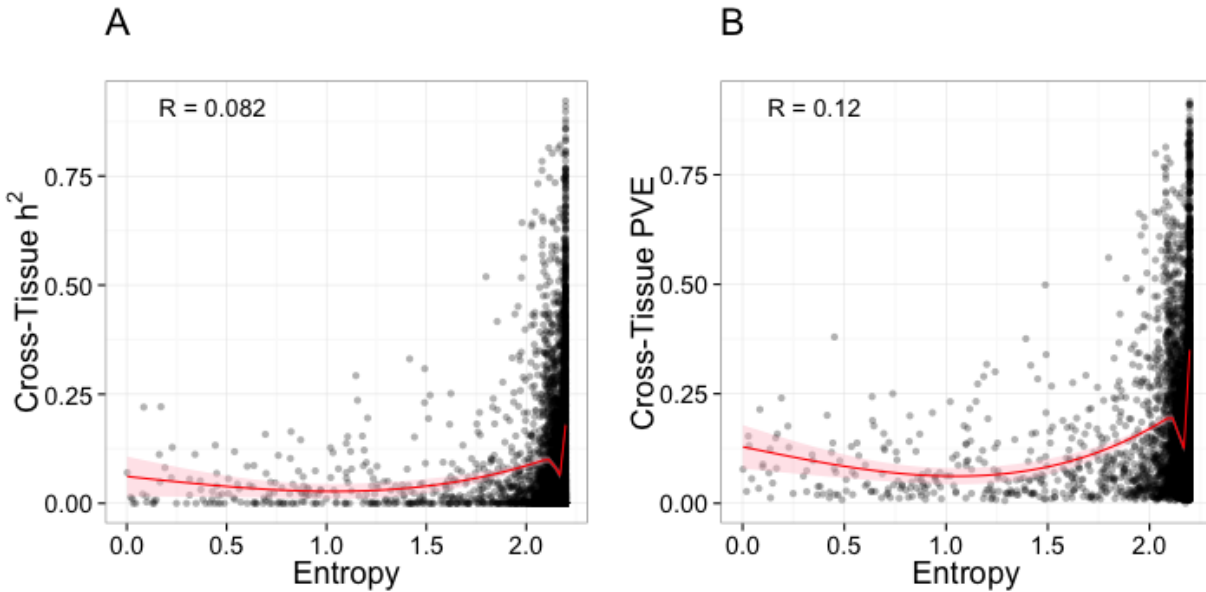


Figure 9: Entropy of the posterior probabilities from the Flutre et al. multi-tissue eQTL method compared to the estimates of (A) heritability and (B) PVE of cross-tissue gene expression derived from the orthogonal tissue decomposition. The generalized additive model smoothing line is in red.

13. Cheung VG, Spielman RS, Ewens KG, Weber TM, Morley M, Burdick JT. Mapping determinants of human gene expression by regional and genome-wide association. *Nature*. Nature Publishing Group; 2005;437: 1365–1369. doi:[10.1038/nature04244](https://doi.org/10.1038/nature04244)
14. Battle A, Mostafavi S, Zhu X, Potash JB, Weissman MM, McCormick C, et al. Characterizing the genetic basis of transcriptome diversity through RNA-sequencing of 922 individuals. *Genome Research*. Cold Spring Harbor Laboratory Press; 2013;24: 14–24. doi:[10.1101/gr.155192.113](https://doi.org/10.1101/gr.155192.113)
15. Ardlie KG, Deluca DS, Segre AV, Sullivan TJ, Young TR, Gelfand ET, et al. The genotype-tissue expression (GTEx) pilot analysis: Multitissue gene regulation in humans. *Science*. American Association for the Advancement of Science (AAAS); 2015;348: 648–660. doi:[10.1126/science.1262110](https://doi.org/10.1126/science.1262110)
16. Gamazon ER, Wheeler HE, Shah KP, Mozaffari SV, Aquino-Michaels K, Carroll RJ, et al. A gene-based association method for mapping traits using reference transcriptome data. *Nature Genetics*. Nature Publishing Group; 2015;47: 1091–1098. doi:[10.1038/ng.3367](https://doi.org/10.1038/ng.3367)
17. Regression shrinkage and selection via the lasso on jSTOR [Internet]. <http://www.jstor.org/stable/2346178>; 2015. Available: <http://www.jstor.org/stable/2346178>

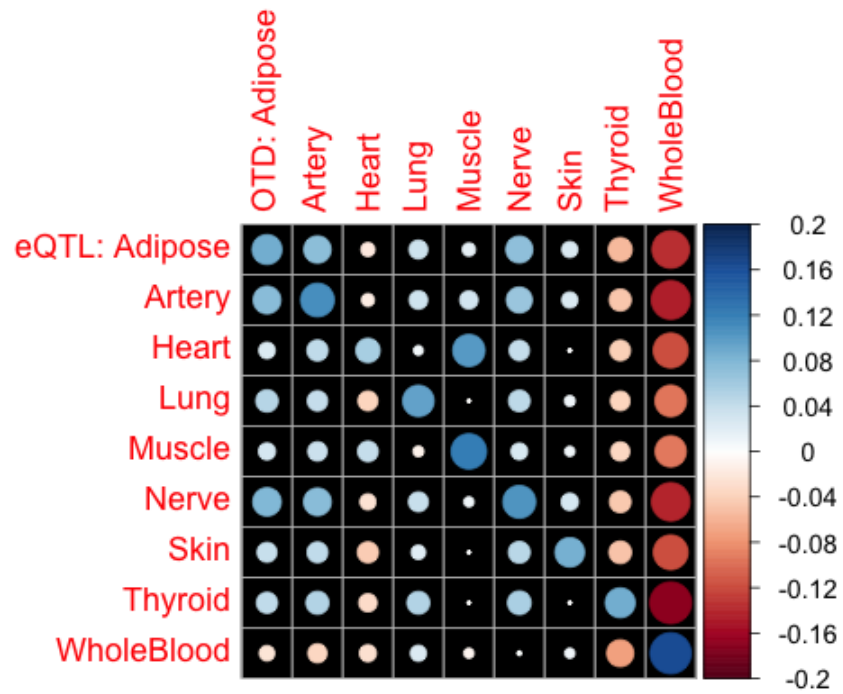


Figure 10: Pearson correlation ( $R$ ) between the posterior probability the top multi-tissue eQTL regulates its gene in a given tissue (eQTL, Flutre et al. method) and the PVE of tissue-specific gene expression from the orthogonal tissue decomposition (OTD). Area of each circle is proportional to the absolute value of  $R$ .

18. Hoerl AE, Kennard RW. Ridge regression: Applications to nonorthogonal problems. *Technometrics*. Informa UK Limited; 1970;12: 69–82. doi:[10.1080/00401706.1970.10488635](https://doi.org/10.1080/00401706.1970.10488635)
19. de los Campos G, Gianola D, Allison DB. Predicting genetic predisposition in humans: The promise of whole-genome markers. *Nat Rev Genet*. Nature Publishing Group; 2010;11: 880–886. doi:[10.1038/nrg2898](https://doi.org/10.1038/nrg2898)
20. Wheeler HE, Aquino-Michaels K, Gamazon ER, Trubetskoy VV, Dolan ME, Huang RS, et al. Poly-omic prediction of complex traits: OmicKriging. *Genetic Epidemiology*. Wiley-Blackwell; 2014;38: 402–415. doi:[10.1002/gepi.21808](https://doi.org/10.1002/gepi.21808)
21. Zhou X, Carbonetto P, Stephens M. Polygenic modeling with bayesian sparse linear mixed models. Visscher PM, editor. *PLoS Genetics*. Public Library of Science (PLoS); 2013;9: e1003264. doi:[10.1371/journal.pgen.1003264](https://doi.org/10.1371/journal.pgen.1003264)
22. Flutre T, Wen X, Pritchard J, Stephens M. A statistical framework for joint eQTL analysis in multiple tissues. Gibson G, editor. *PLoS Genetics*. Public Library of Science (PLoS); 2013;9: e1003486. doi:[10.1371/journal.pgen.1003486](https://doi.org/10.1371/journal.pgen.1003486)
23. Yang J, Lee SH, Goddard ME, Visscher PM. GCTA: A tool for genome-wide complex trait analysis. *The American Journal of Human Genetics*. Elsevier BV; 2011;88: 76–82. doi:[10.1016/j.ajhg.2010.11.011](https://doi.org/10.1016/j.ajhg.2010.11.011)
24. Zhang X, Joehanes R, Chen BH, Huan T, Ying S, Munson PJ, et al. Identification of common genetic variants controlling transcript isoform variation in human whole blood. *Nature Genetics*. Nature Publishing Group; 2015;47: 345–352. doi:[10.1038/ng.3220](https://doi.org/10.1038/ng.3220)
25. Zou H, Hastie T. Regularization and variable selection via the elastic net. *Journal of the Royal Statistical Society: Series B (Statistical Methodology)*. Wiley-Blackwell; 2005;67: 301–320. doi:[10.1111/j.1467-9868.2005.00503.x](https://doi.org/10.1111/j.1467-9868.2005.00503.x)
26. Howie B, Fuchsberger C, Stephens M, Marchini J, Abecasis GR. Fast and accurate genotype imputation in genome-wide association studies through pre-phasing. *Nature Genetics*. Nature Publishing Group; 2012;44: 955–959. doi:[10.1038/ng.2354](https://doi.org/10.1038/ng.2354)
27. Fuchsberger C, Abecasis GR, Hinds DA. Minimac2: Faster genotype imputation. *Bioinformatics*. Oxford



University Press (OUP); 2014;31: 782–784. doi:[10.1093/bioinformatics/btu704](https://doi.org/10.1093/bioinformatics/btu704)

28. Harrow J, Frankish A, Gonzalez JM, Tapanari E, Diekhans M, Kokocinski F, et al. GENCODE: The reference human genome annotation for the ENCODE project. *Genome Research*. Cold Spring Harbor Laboratory Press; 2012;22: 1760–1774. doi:[10.1101/gr.135350.111](https://doi.org/10.1101/gr.135350.111)

29. Friedman J, Hastie T, Tibshirani R. Regularization paths for generalized linear models via coordinate descent. *Journal of Statistical Software*. 2010;33: 1–22. Available: <http://www.jstatsoft.org/v33/i01/>

30. Simon N, Friedman J, Hastie T, Tibshirani R. Regularization paths for cox’s proportional hazards model via coordinate descent. *Journal of Statistical Software*. 2011;39: 1–13. Available: <http://www.jstatsoft.org/v39/i05/>

31. Zhou X, Stephens M. Genome-wide efficient mixed-model analysis for association studies. *Nature Genetics*. Nature Publishing Group; 2012;44: 821–824. doi:[10.1038/ng.2310](https://doi.org/10.1038/ng.2310)

32. Im HK, Gamazon ER, Stark AL, Huang RS, Cox NJ, Dolan ME. Mixed effects modeling of proliferation rates in cell-based models: Consequence for pharmacogenomics and cancer. Akey JM, editor. *PLoS Genetics*. Public Library of Science (PLOS); 2012;8: e1002525. doi:[10.1371/journal.pgen.1002525](https://doi.org/10.1371/journal.pgen.1002525)

33. R Core Team. R: A language and environment for statistical computing [Internet]. Vienna, Austria: R Foundation for Statistical Computing; 2015. Available: <http://www.R-project.org/>

34. Bates D, Maechler M, Bolker B, Walker S. lme4: Linear mixed-effects models using eigen and s4 [Internet]. 2014. Available: <http://CRAN.R-project.org/package=lme4>

35. Bates D, Maechler M, Bolker BM, Walker S. lme4: Linear mixed-effects models using eigen and s4 [Internet]. 2014. Available: <http://arxiv.org/abs/1406.5823>

36. Stegle O, Parts L, Piipari M, Winn J, Durbin R. Using probabilistic estimation of expression residuals (PEER) to obtain increased power and interpretability of gene expression analyses. *Nat Protoc*. Nature Publishing Group; 2012;7: 500–507. doi:[10.1038/nprot.2011.457](https://doi.org/10.1038/nprot.2011.457)